Investigation on the Mechanical, and third harmonic generation analyses of non-linear optical single crystal of 2-Phenyl benzimidazole

A. Muthuraja[1*], J. Sivasankari[1], S. Swetha[1], K. Gurupriya[1], L. Kiruthika[1]

*[*1]Department of Physics, Theivanai Ammal College for Women (Autonomous),*
Villupuram – 605 602. Tamilnadu, India.
Email Address: *amuthuraja90@gmail.com*

Abstract

The slow evaporation solution growth technique is used to grow single crystals of 2-phenylbenzimidazole (2PBMZ). The crystal is belongs to the monoclinic system with space group C2/c, which is revealed through the single crystal XRD. The cut-off wavelength and optical band gap energy of the 2PBMZ crystal were observed at 568 nm and 1.96 eV respectively. The Vickers (Hv) hardness number, yield strength and stiffness constant are calculated, which is found to increase with the applied load. The Z-scan technique with He–Ne laser (632.8 nm) has used to study the third order nonlinear optical property of 2PBMZ crystal.
Key words: Crystal growth, Vickers Microhardness, Z-Scan.

1. Introduction

In recent years, researchers show more interest towards organic materials due to its probable applications in frequency conversion, telecommunication, optical information processing, and high optical disk data storage [1]. The organic materials are more non-linear when compared to inorganic materials due to its bonds and weak Vander Waal's nature, which result in high degree of delocalization [2]. The organic materials show prominent properties due to their fast and large nonlinear response over a broad frequency range, inherent synthetic flexibility, and large optical damage threshold [3]. All these superior properties of the organic non-linear (NLO) materials attract the interest of researchers, rather than inorganic materials. The organic π-conjugated materials with strong optical nonlinearities can be easily refrained by molecular design. Such material shows an effective output in all-optical device applications [4]. The title material is a benzimidazole derivative. The very essential thing for the fabrication of devices is hardness measurement [5]. Muthuraja et al. [6] reported the growth, structural and optical properties of 2PBMZ single crystals using Solution growth method and it was compared with other benzimidazole derivatives. There is no information available on depth analysis of mechanical properties such as Knoop measurement, Stiffness constant, Resistance pressure plot, yield strength and third harmonic generation. In the present investigation, we have reported the mechanical analysis with different kind of analysis, photoconductivity, and third harmonic generation. In addition to that, the powder XRD and UV–Vis–NIR studies of 2PBMZ single crystal were also carried out.
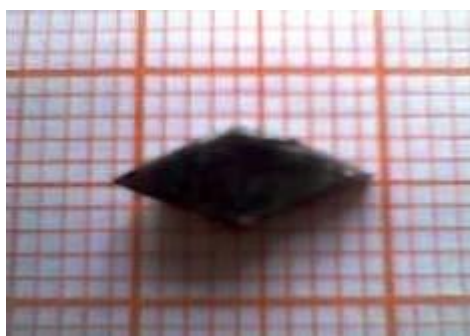
2. Experimental procedure

Fig.1 As grown crystal

The 2PBMZ with 99% purity was commercially purchased from Sigma Aldrich. The 2PBMZ is highly soluble in N-N-dimethylformamide. The 0.017 mole of 2-phenylbenzimidazole was dissolved in 20ml of solvent at room temperature. The saturated solution was prepared and filtered. The filtered solution is allowed to evaporate and the slow evaporation solution growth technique was use to grow single crystals within a period of 30 days. The grown crystals are Rhombohedra in shape and black in colour. The dimension of the grown crystal is 10x4x2 mm^3. Fig. 1 shows the grown 2PBMZ single crystals.

3. Result and discussion
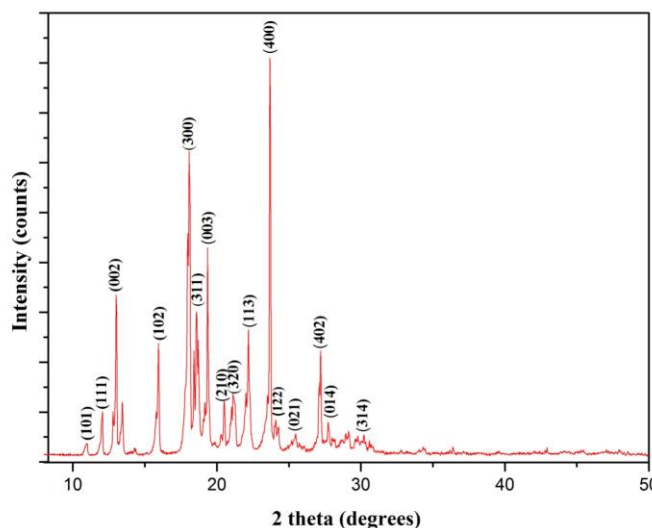
3.1 X-ray diffraction analysis

Fig. 2 Powder XRD spectrum

At room temperature, the 2PBMZ single crystal was subjected to single crystal X-ray diffraction study and it is found that the grown crystal is belongs to monoclinic system with Centro symmetric space group C2/c. The lattice parameters are a=22.303 Å, b=7.303 Å, c=5.341 Å; $\alpha=\gamma=90^O$ and $\beta=91.58^O$, and the cell volume is 869.6 Å^3. The crystal was finely powdered and subjected to powder X-ray diffraction analysis and the values are recorded in the 2θ ranging from 20 - 70º. The grown 2PBMZ crystal shows the good crystalline nature, which is clearly observed from the diffraction peaks. The powder XRD pattern of 2PBMZ crystal was shown in Fig. 2. The unit cell parameters of 2PBMZ are in good agreement with reported values [7].
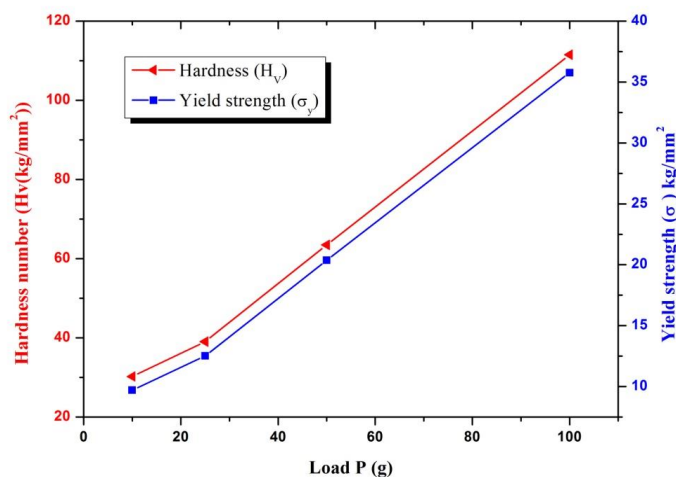
3.2 Microhardness measurements.

Fig 3. Hardness and yield strength with applied load,

The hardness is the most domineering mechanical property of the crystal among several other properties. The hardness of the crystal is used to determine the mechanical stability of the crystal, which is an undeniable parameter [8]. The Mututoyo MH-112 micro hardness tester was used to carry out the hardness measurement. The dimension of the sample used for the hardness measurement is $10 \times 4 \times 2 mm^3$. The Indentation was applied on the polished surface of the crystal with indentation time of 10s. The measurements were carried out for various loads ranging from 10 to 100 gm which shown in Fig 3. The hardness number increases with an increase in applied load, which is due to the reverse indentation size effect [9]. The Vickers Micro hardness number (Hv) of the crystal was calculated using the standard formula

$$H_v = 1.8544 \, P/d^2 \, .$$

Where P is the load applied in kg, d in mm. H_v is the Vickers hardness number in kg/mm^2. When the applied load reaches 100 gm, the crack starts to occur on the surface of the crystal, which is due to the release of internal stresses generated locally by indentation [10].
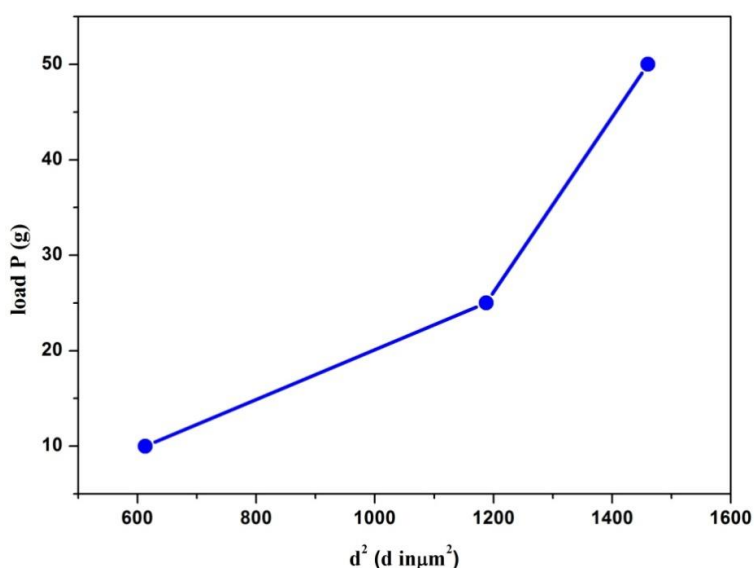
3.4 Hays-Kendall's approach

Fig. 4. Resistance pressure plot.

According to Hays – Kendall approach [11]. $P = W + A_1 d^2$, Where W is the minimum load to initiate plastic deformation and A_1 is a load independent constant. Fig. 4 shows the graph plotted between the values of P and d^2. The value of W is the intercept along the load axis and A_1 is the slope. The corrected hardness H_0 for the crystal has been estimated using the following relation $H_o = 1854 \times A_1$. The negative value of constant W indicates that the crystals are exhibiting the strongly behaviour of reverse ISE. The values of W and Ho were calculated and tabulated (Table 1).

Table . 1 2-PBMZ crystal Calculated value of W, A_1 and H_o

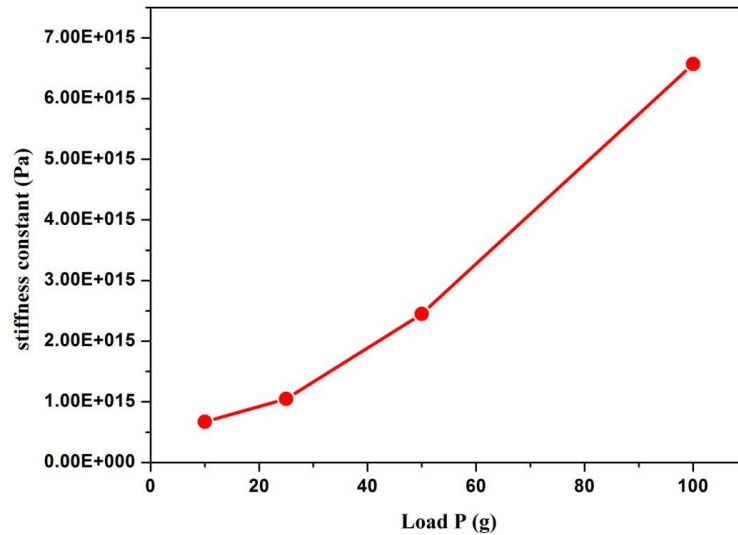| Hays–Kendall approach	2-PBMZ Crystal
Resistance pressure (W)	-19.42093 (g)
Load independent constant (A1)	0.04394 (g μm^{-2})
Corrected hardness (Ho)	81.4647(g μm^{-2})

Fig. 5. Stiffness constant

The elastic stiffness constant (C_{11}) gives an idea of the tightness of bonding between the neighbouring atoms. The stiffness constant increases with an increase in load which is clearly shown in Fig. 5. The Wooster's empirical relation $C_{11} = H_v^{7/4}$ was used to derive the elastic stiffness constant for different loads. It gives an idea about the tightness of bonding between neigh boring atoms [12]. The hardness value was used to derive the yield strength (σ_y) by using the following equation [13]. From a Meyer index value $n > 2$ (2.1), the yield strength σ_y was calculated using the expression. Fig. 3 clearly reveals that the yield strength increases with an increase in applied load.

$$\sigma_y = \frac{H_v}{2.9}[1-(n-2)]\left(\frac{12.5(n-2)}{1-(n-2)}\right)^{n-2}$$

The values of yield strength and elastic stiffness constant were calculated with various loads and tabulated in the table 2.

Table 2: Microhardness, yield strength, and elastic stiffness constant values of 2-PBMZ

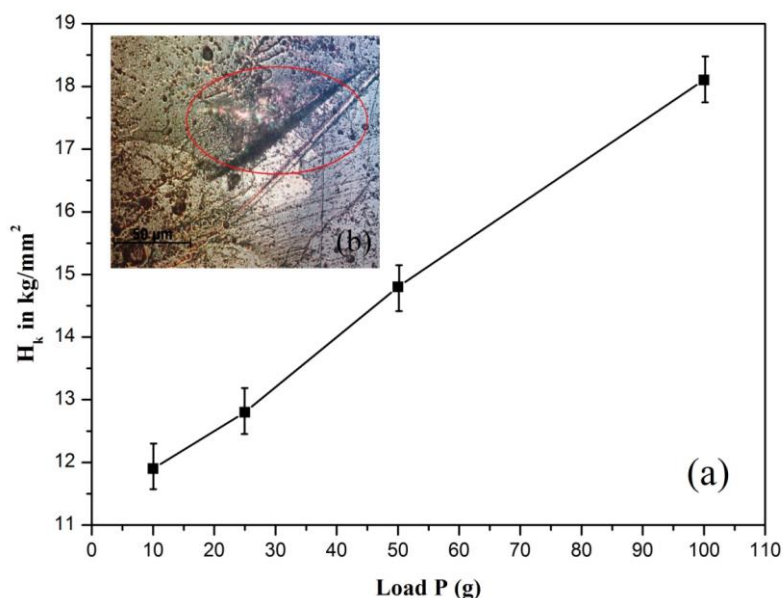| S.No	Load P (g)	Hv (kg mm^2)	Yield Strength σy (kg/mm^2)	Elastic stiffness constant C_{11} x 10^{15} (Pa)
1	10	30.26060156	9.70484982	6.70164
2	20	39.04027616	12.52057122	1.04663
3	50	63.4900538	20.36183702	2.45121
4	100	111.5087573	35.76187144	6.56805

3.5

Knoop measurement

Fig. 6. (a) Knoop measurement, (b) Knoop indentation

When the applied load increases up to 100 g, the Knoop microhardness number also increases. This is due to the reverse indentation size effect and which is proved from the Knoop hardness measurement [14]. The Knoop hardness number (H_k) was calculated in consideration with the long diagonal length (d) from the following derivation,

$$H_k = 14.229P/ d^2.$$

Fig. 6 (a) shows the graph was plotted for Knoop hardness (H_k) versus load (P). The knoop impression obtained from the Knoop hardness seems in a rhombohedral shape which is shown in Fig 6 (b). The Knoop microhardness Young's modulus was derived from the hardness value using the following relation,

$$E = 0.45H_k / (0.1406 - b/a).$$

Where H_k is the hardness value at a particular load, b and a are the shorter and longer Knoop indentation diagonal respectively. The derived Young's Modulus value is 2.895×10^{12} g/m^2.
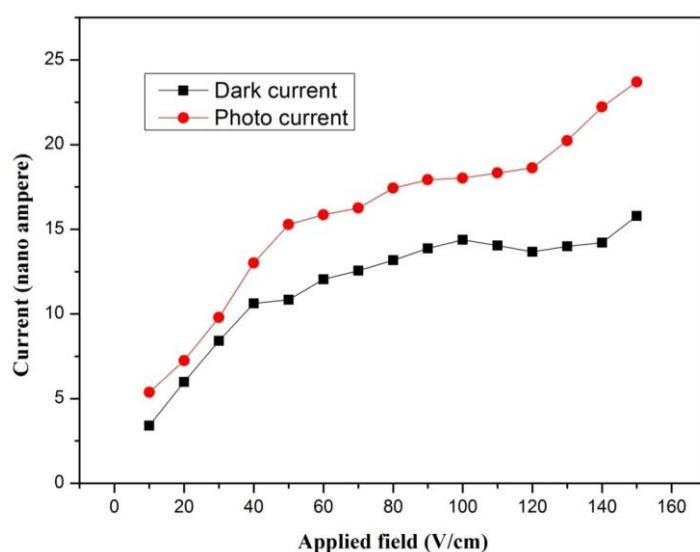
3.6 *Photoconductivity*

Fig. 7. Photo conductivity

The photosensitive materials are most recently used in many latest applications such as military applications, photo detection, communication through fiber optics, radiation measurements and in guided weapons [15, 16]. The photoconductivity was measured using the Keithley 6485 Pico ammeter at room temperature. The voltage power supply and sample was connected with Keithley 6485 Pico-Ammeter in series. The crystal was ignited using the halogen lamp with 100 W applied voltage and the photo current was recorded for the same applied voltage. Along with the electrometer DC supply, the thin copper wire was connected to the opposite faces of the sample crystal. The input voltage was increased from 1 V to 30 V by the steps of 2 V. The applied field was adjusted for both dark and photo currents. The photoconductivity plot depends is shown in Fig. 7. From the graph, it is very clear that both the dark current and photo current increases with the applied field. At the same time, the photo current increases rapidly than the dark current. This condition is termed as positive photo conductivity. Materials with the positive photo conductivity behaviour are used for soliton wave communications [17].
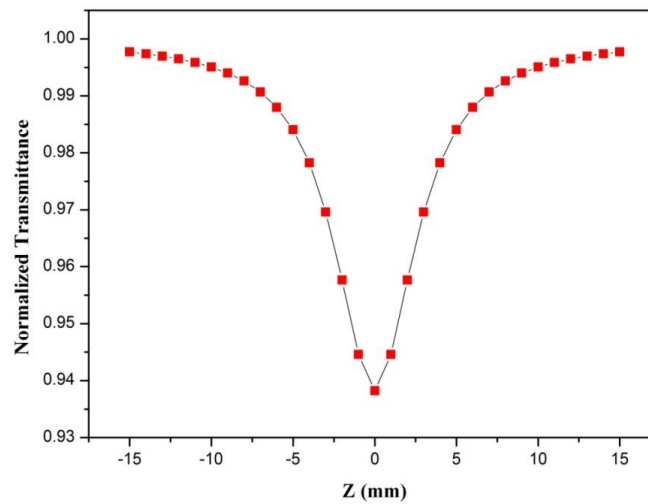
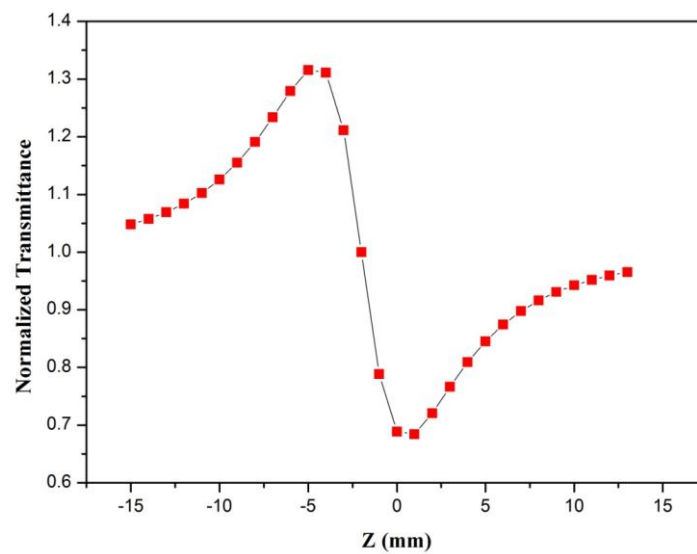### 3.8 Z-scan Analysis

Fig. 8 open aperture

Fig. 9 Closed apertures

When compared to other measurement techniques like nonlinear refraction interferometer, ellipse rotation, beam distortion measurements, degenerate four wave mixing and three wave mixing, the Z-scan technique is very easy and efficient technique [18]. Both the non-linear absorption and refraction of crystals can be clearly defined from the Z-scan technique, than the thin films and liquid solutions established by shakebahae et.al. The Z-scan technique is very laid-back to understand, so this method was agree to take by non-linear optics community. It is used to quantity both the non-linear refractive index and non-linear absorption coefficient. The two main basic factors behind the Z-scan technique is self-focusing and self-defocusing [19]. In this current experiment, the third-order NLO properties of the title crystal were measured using the He–Ne laser (5 mW), in which the laser possess the wavelength and beam diameter of 632.8 nm and 0.5 mm respectively. The Gaussian filter was used to convert the input laser beam in to the Gaussian form. The Gaussian beam was allowed to pass through the convex lens with the focal length of 30 mm, in which the focal length mainly depends on the incident Gaussian beam. The diameter of the Gaussian beam waist ω0 at the focal length was 12.05 mm. The sample was transitioned from +Z to - Z axial direction using stepper motor, and also to regulate the incident intensity falling on the crystal surface. The far field transmittance intensity variation in a closed aperture method was measured using the digital power meter (Field master GS-coherent). On the other hand, the refracted laser beam was entirely placid in the detector in an open aperture method which is shown in fig. 8. The size of the aperture decreased in terms of the diameter of the laser beam at the closed aperture method. Fig. 9 reveals self-defocusing effect at the closed aperture method. The self-defocusing effect upsurges the beam divergence which directly leads to broadening of beam at the focal length. The saturation absorption enriches the peak and surmounts the valley at the focal point of the optical path and it is vice versa in the case of multi-photon absorption [20]. The effective non-linear optical property of the grown crystal makes it an auspicious material for optical limiting applications. The experimental results and details of the 2PBMZ crystal are tabulated in Table 3.

Table 3. The experimental results and details of the 2PBMZ crystal are tabulated

Measurement details of Z-Scan experiment	
Laser beam wavelength (λ)	632.8 nm
Focal length of lens	30 mm
Optical path length	75 cm
Beam radius of the aperture (w_a)	3.5 mm
Aperture radius (r_a)	1mm
Sample thickness (L)	1.07 mm
Beam radius (Wo)	6.03×10^{-6}
Effective thickness (L_{eff})	0.153004978 mm
Linear absorption coefficient (α)	6.5296959
Linear transmittance (S)	0.150634
Nonlinear refractive index (n_2)	3.97×10^{-11} m^2/W
Nonlinear absorption coefficient (β)	2.74×10^{-4} m/W
Real part of third order susceptibility [Re(χ3)]	2.65237×10^{-5} esu
Imaginary part of third order susceptibility [Im(χ3)]	9.24315×10^{-6} esu
Third order nonlinear susceptibility (χ3)	2.8088×10^{-5} esu

4. Conclusion

The slow evaporation technique was used to grow the 2-phenyl benzimidazole (2PBMZ) single crystals successfully. The reverse indentation size effect is observed in the grown single crystals. The elastic stiffness

constant (C_{11}) and yield strength (σv) of the grown crystal were derived. From the stiffness constant value of the crystal, this is found that the binding forces between the ions are very strong. The Young's modulus value of the crystal was calculated from the diagonal lengths of the Knoop indentation. The nonlinear refractive index and nonlinear susceptibility of 2PBMZ single crystals are calculated from Z-scan measurements.

Acknowledgement

References

[1] Arunkumar A, and Ramasamy P, *Material letter* 123 (2014) 246.

[2] Santhakumari R, Ramamurthi K, Vasuki G, Yamin B.M, and Bhagavannarayana G, *Spectrochim. Acta, Part A* 76 (2010) 369.

[3] Lin JT, Wang WS, and Arend H, *Proc SPIE* 100 (1989)1104.

[4] Hales J.M, Matichak J, Barlow S, Ohira S, Yesudas K, Bredas J.L, Perry J.W, and Marder S.R, *Science,*327 (2010) 1485.

[5] Amirdha Sher Gill, and Kalainathan S, *Mater Lett* 65 (2011) 53.

[6] Muthuraja A, and Kalainathan S. *Materials Technology* 32:6, (2016) 335-348.

[7] Javier Zuniga F. Lukas Palatinus, Pilar Cabildo, Rosa M. Claramunt and Jose Elguero, Z. *Kristallogr.* 221 (2006) 281.

[8] Subramaniyan@Raja R, AnandhaBabu G, and Ramasamy P, *J. Cryst. Growth* 334 (2011) 159.

[9] Muthuraja, A. Kalainathan S, Journal of Crystal Growth 459 (2017) 31–37.

[10] Felicita Vimala J, Lawrence M, Joseph Prakash J.T, and Elixir. *Cryst.Growth*. 41 (2011) 5664

[11] Hays. C, Kendall, E.G. Metallography 6 (1973) 275.

[12] Nirosha M. Kalainathan S, Sarveswari S, and Vijayakumar V. *Spectrochim Acta Part A* 123 (2014) 78.

[13] Senthil K. Kalainathan S. Ruban Kumara A, and Aravindan P. G. *RSC Adv.,* 4, (2014) 56112.

[14] Sangwal K. *Cryst Res Technol* 44 (2009)1019.

[15] Bube R.H, *Wiley Interscience*, *New York,* (1960)

[16] Milton Boaz B, Samuel Selvaraj R, Senthil Kumar K, and Jerome Das S. *Indian J. Phys.* 83(2009) 164.

[17] Milton Boaz B, Mary Navis Priya S, Mary Linet L, Martin Deva Prasath P, and Jerome Das S, *Opt. Mater.* 29 (2007) 827.

[18] Sheik-bahae M, Said A.A, Wei T, Hagan D.J, and Van stryland E.W. *IEEE J. Quantum Electron*. 26 (1990) 4.

[19] Nirosha M, Kalainathan S, Sarveswari S, Vijayakumar V, and Srikanth A. S*pectrochimica Acta Part A: Molecular and Biomolecular Spectroscopy* 13(2015) 723.

[20] Bharath D, and Kalainathan S. *Spectrochimica Acta Part A: Molecular and Biomolecular Spectroscopy* 118 (2014) 1098.